

Synthesis and Characterization of a $[\text{Mn}_{12}\text{O}_{12}(\text{O}_2\text{CR})_{16}(\text{H}_2\text{O})_4]$ Complex Bearing Paramagnetic Carboxylate Ligands. Use of a Modified Acid Replacement Synthetic Approach

Philippe Gerbier¹, Daniel Ruiz-Molina¹, Neus Domingo²,
David B. Amabilino¹, José Vidal-Gancedo¹, Javier Tejada²,
David N. Hendrickson³, and Jaume Veciana^{1,*}

¹ Institut de Ciència de Materials de Barcelona (CSIC), Campus UAB, E-08193,
Cerdanyola, Spain

² Facultat de Física, Universitat de Barcelona, E-08028 Barcelona, Spain

³ Department of Chemistry and Biochemistry-0358, University of California at San Diego,
La Jolla, California 92093-0358, USA

Received March 27, 2002; accepted May 2, 2002

Published online September 2, 2002 © Springer-Verlag 2002

Summary. A new modified approach for the synthesis of Mn_{12} clusters, based on the use of complex $[\text{Mn}_{12}\text{O}_{12}(\text{O}_2\text{C}^t\text{Bu})_{16}(\text{H}_2\text{O})_4]$ (**2**) as starting material to promote the acidic ligand replacement, is presented here. This new synthetic approach allowed us to obtain complex $[\text{Mn}_{12}\text{O}_{12}(\text{O}_2\text{CC}_6\text{H}_4\text{N}(\text{O}^\bullet)^t\text{Bu})_{16}(\text{H}_2\text{O})_4]$ (**3**), whose preparation remained elusive by direct replacement of the acetate groups of Mn_{12}Ac (**1**). Complex **3** bearing open-shell radical units, was prepared to increase the total spin number of its ground state, and consequently, to increase T_B , with the expectation that the radical ligands may couple ferromagnetically with the Mn_{12} core. Unfortunately, magnetic measurements of complex **3** revealed that the sixteen radical carboxylate ligands interact antiferromagnetically with the Mn_{12} core to yield a $S = 2$ magnetic ground state.

Keywords. Single-Molecule Magnet; Synthesis; Paramagnetic ligand; Pivalic acid.

Introduction

The rapid growth of high-speed computers and the miniaturization of magnetic technology have led to much interest in the field of nanoscale magnetic materials [1–3]. In the past decade, the data density for magnetic hard disk drives has

* Corresponding author. E-mail: vecianaj@icmab.es

increased at a phenomenal pace: doubling every 18 months and, since 1997, doubling every year, which is much faster than the *Moore's Law* for integrated circuits. To maintain such miniaturization rates constantly, the development of new technologies based on lithographic and scanning probe microscopies, the so-called *top-down* approach, have been greatly enhanced. However, the ever-increasing demand of higher areal density magnetic storage media may find technological and economical limitations in a near future. Moreover, the continuous miniaturization of magnetic materials may lead to the observation of new phenomenologies such as superparamagnetic effects or quantum behavior.

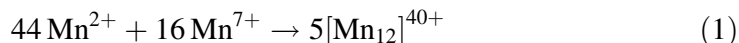
The use of synthetic methodologies, the so-called *bottom-up* approach, offers a potential alternative to obtain monodispersed nanoscale magnetic materials of a sharply defined size. The discovery of large metal cluster complexes with interesting magnetic properties characteristic of nanoscale magnetic particles, such as out-of-phase ac magnetic susceptibility signals and stepwise magnetization hysteresis loops, represented an exciting breakthrough to access ultimate high-density information storage devices and quantum computing applications.

In 1993 it was discovered for the first time that $[\text{Mn}_{12}\text{O}_{12}(\text{O}_2\text{CCH}_3)_{16}(\text{H}_2\text{O})_4] \cdot 4\text{H}_2\text{O} \cdot 2\text{CH}_3\text{CO}_2\text{H}$ (**1**), functions as a nanoscale molecular magnet and for this reason the term of Single-Molecule Magnet (SMM) was coined [4, 5]. Since then, a few more families of complexes that function as SMM's have been obtained including several other structurally related neutral or negatively charged dodecanuclear manganese complexes, $[\text{Mn}_{12}\text{O}_{12}(\text{O}_2\text{CR})_{(16-X)}\text{L}_X(\text{H}_2\text{O})_4]$, commonly known as Mn_{12} , where R can be a saturated or an unsaturated organic group and L a diphenylphosphinate ligand or a nitrate anion [6–11], Mn_4 mixed-valence cubane molecules [12, 13], tetranuclear vanadium(III) complexes with a butterfly structure [14, 15] and iron(III) complexes such as $[\text{Fe}_8\text{O}_2(\text{OH})_{12}(\text{tacn})_6]^{8+}$ [16, 17] and $[\text{Fe}_4(\text{OMe})_6(\text{dpm})_6]$ [18] where *tacn* and *dpm* stand for 1,4,7-triazacyclononane and dipivaloylmethane respectively.

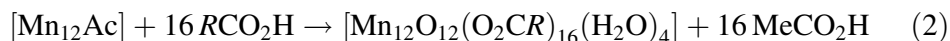
Even though different families of SMMs have been synthesized (*vide supra*), all of them show low blocking temperatures (T_B) above which they behave as superparamagnets. The highest T_B (*ca.* 6 K) so far reported corresponds to the Mn_{12} family. Mn_{12} complexes can be described as a $[\text{Mn}_{12}(\mu_3\text{-O})_{12}]$ core comprising a central $[\text{Mn}^{\text{IV}}_4\text{O}_4]^{8+}$ cubane unit held within a nonplanar ring of eight Mn^{III} ions by eight $\mu_3\text{-O}^{2-}$ ions. Peripheral ligation is provided by sixteen carboxylate groups and three or four H_2O ligands. As a consequence, Mn_{12} complexes have a high-spin ground state $S = 10$, which can be understood assuming that the Mn^{IV} ($S = 3/2$) of the central $[\text{Mn}^{\text{IV}}_4\text{O}_4]^{8+}$ cubane are aligned with all the spins down that interact antiferromagnetically with all the Mn^{III} ($S = 2$) of the external ring with all spin aligned up. Moreover, the strong uniaxial magnetic anisotropy of the molecule originated by the single-ion zero field splitting experienced by the Mn^{III} ions splits the $S = 10$ ground state into the different $m_s = \pm 10, \pm 9, \pm 8, \pm 7, \dots, 0$ levels. In zero field, the $m_s = 10$ levels are the lowest in energy followed by 9, 8, 7, ... at higher energies and $m_s = 0$ is the highest energy. Then, an energy barrier for the interconversion from the *spin up* to the *spin down* state of the complex appears and slow magnetization relaxation processes are observed. Such barrier is the responsible of the SMM behavior of the Mn_{12} family.

There are basically two different synthetic procedures available for making new $[\text{Mn}_{12}\text{O}_{12}(\text{O}_2\text{CR})_{16}(\text{H}_2\text{O})_4]$ complexes [19]. The first involves the

comproportionation between a Mn^{II} source and Mn^{VII} from MnO_4^- in the presence of the desired carboxylic acid (RCOOH). This was the original method used by *Lis* [20] to synthesize complex **1**.



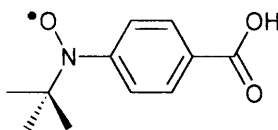
In the second synthetic approach, a variety of derivatives have been prepared by ligand substitution reactions, which are driven by the greater acidity of the added carboxylic acids RCO_2H and/or the removal by distillation of an azeotrope of acetic acid and toluene (see Eq. 2).



It has to be emphasized that several treatments with the new carboxylic acid are sometimes needed to replace all acetate groups. The advantage is that reaction yields are generally larger than those obtained in the first approach.

More recently, a new functionalization of Mn_{12} SMM with ligands other than carboxylate or site-specific modifications to yield mixed-carboxylate $[\text{Mn}_{12}\text{O}_{12}(\text{O}_2\text{CR})_8(\text{O}_2\text{CR}')_8(\text{H}_2\text{O})_4]$ complexes, have been achieved [8, 9]. The interest for the development of these new synthetic methodologies lies in the variety of reactivity studies and applications that can be achieved with an intrinsic SMM behavior.

In this work, we present a modification of the synthetic route shown in Eq. 2 for the convenient synthesis of a large variety of already known and new manganese complexes. Such modification, which is based on the use of complex $[\text{Mn}_{12}\text{O}_{12}(\text{O}_2\text{C}^t\text{Bu})_{16}(\text{H}_2\text{O})_4]$ (**2**), as starting material for the substitution reaction, may possess several advantages: *i*) the presence of *tert*-butyl groups instead of methyl groups at the periphery of the Mn_{12} core should increase significantly its solubility in organic solvents, *ii*) the steric compression afforded by the presence of the bulky *tert*-butyl groups should help the substitution by less bulky acids, and *iii*) when compared with other carboxylic acids, the dissociation constant of the pivalic acid also should favor the displacement of the substitution equilibrium to completion [21]. In short, this approximation is expected to favor the formation of new and exotic Mn_{12} SMMs otherwise unrealizable by direct replacement of the acetate groups of Mn_{12}Ac (**1**). As an experimental example for the convenience of this new synthetic route we report here the synthesis and characterization of the new Mn_{12} complex $[\text{Mn}_{12}\text{O}_{12}(\text{O}_2\text{CC}_6\text{H}_4\text{N}(\text{O}^\bullet)^t\text{Bu})_{16}(\text{H}_2\text{O})_4]$ (**3**), which has the 1-[*N-tert*-butyl-*N*-(oxyl)amino]-4-benzoic acid radical (**4**) in the peripheral ligation. All the attempts to synthesize complex **3** by direct replacement of the acetate groups of Mn_{12}Ac (**1**) invariably afforded ill-defined products whose preliminary analyses showed large amounts of Mn^{2+} ions. The interest to obtain such complex is clear; the open-shell character of the radical carboxylate ligands was expected to increase the high-spin ground state value in the most favorable case of a ferromagnetic interaction between the ligands and the Mn_{12} core, and consequently, to increase the blocking temperature T_B of the SMM.



Results and Discussion

Synthesis

Complex **2** was synthesized according to the conventional synthetic approach shown in Eq. 2 and fully characterized by elemental analysis, LDI/MALDI-TOF mass spectroscopy, FT-IR and UV-Vis spectroscopy, and SQUID measurements. To a slurry of complex **1** was added an excess of pivalic acid ($\text{HO}_2\text{C}^t\text{Bu}$) and the resulting solution was allowed to stir overnight. Then, the mixture was concentrated under vacuum to remove the acetic acid. To fully substitute the acetate ligands, this procedure was repeated once more, yielding a microcrystalline material that was satisfactorily characterized as complex **2**. In contrast to **1**, which is poorly soluble, complex **2** is quite soluble in non polar organic solvents such as hexane, although it may be recrystallized from polar solvents such as acetonitrile. However, in spite of repeated efforts, no crystals suitable for X-ray structural determination were obtained.

^1H NMR spectroscopy was used to follow the formation of complex **2**. The ^1H NMR spectrum of a solution of complex **1** in deuterated acetonitrile, displays resonances at $\delta = 48.2$, 41.8 and 13.9 ppm with a 1:2:1 relative intensity. These signals have been ascribed to axial methyl groups linked to two Mn^{III} , equatorial methyl groups linked to one Mn^{III} and axial methyl groups linked to one Mn^{IV} , respectively. In the same solution, an excess of pivalic acid (1:40) was added and its evolution with time was monitored. According to the spectrum recorded after 20 min of reaction, an extensive ligand exchange reaction took place. The ligand exchange reaction was continued for 10 additional hours although no further changes were noticed in the corresponding ^1H NMR spectra, indicating that the exchange equilibrium has been reached at an early stage of the reaction.

The spectrum of a solution of complex **2** is shown in Fig. 1. The *tert*-butyl groups are split into three sets of resonances centered at $\delta = 11.6$, 5.0, and -2.0 ppm in a relative ratio of 1:1:2, the latter being further split into a triplet. The additional resonance at $\delta = 15.3$ ppm was ascribed to the coordinated water molecules.

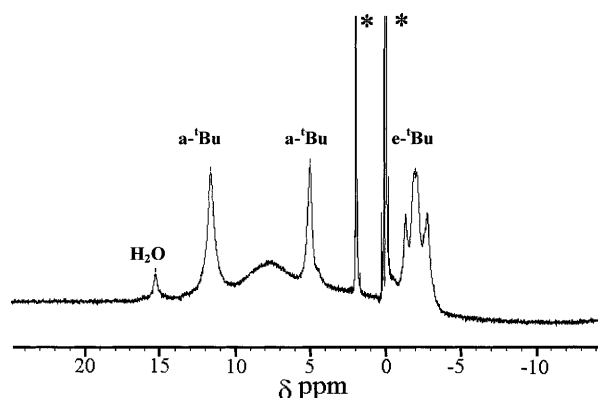


Fig. 1. ^1H NMR spectrum of a CD_3CN solution of complex $[\text{Mn}_{12}\text{O}_{12}(\text{O}_2\text{C}^t\text{Bu})_{16}(\text{H}_2\text{O})_4]$ **2**. Signals associated to solvent and TMS, when present, are marked with an asterisk; a = axial, e = equatorial

As described recently this spectrum is consistent with an effective D_{2d} molecular symmetry in solution [9]. This makes the eight equatorial $t\text{-BuCO}_2$ groups virtually equivalent, but the axial groups are of two types. Therefore, the singlets at $\delta = 11.6$ and 5.0 ppm are assigned to axial *tert*-butyl groups whereas the triplet at $\delta = -2.0$ ppm is ascribed to equatorial ones. The multiplicity of the latter peak should arise from the fact that the equatorial groups of Mn_{12} complexes are diastereoscopic [9] giving a 1:2:1 distribution for a *tert*-butyl group. From these experiments, one can firstly assess that the ligand exchange reaction should start with the replacement of the more labile axial carboxylates. Moreover, if we consider both the relative intensity of the peaks at $\delta = 9.6$ and 5.1 ppm (axial $t\text{-Bu}$) observed after 20 min of reaction, and the structures of the mixed ligand $[\text{Mn}_{12}\text{O}_{12}(\text{NO}_3)_4(\text{O}_2\text{CCH}_2t\text{-Bu})_{12}(\text{H}_2\text{O})_4]$ and $[\text{Mn}_{12}\text{O}_{12}(\text{O}_2\text{CCH}_3)_4(\text{O}_2\text{CCH}_2\text{CH}_3)_{12}(\text{H}_2\text{O})_4]$ complexes [9], one can secondly assess that the resonance at ca. 10 ppm, which is the more prominent, should be ascribed to the axial pivalate ligands linked to two Mn^{III} . Finally, if we consider that these four axial positions are fully occupied by pivalate ligands, this gives for the pivalate ligands an occupancy of 0.25 for the four remaining axial positions (linked to one Mn^{III} and one Mn^{IV}) and an occupancy of 0.50 for the eight equatorial positions at the exchange equilibrium.

As previously mentioned, direct reaction of the acidic radical **4** with the Mn_{12}Ac complex yielded different ill-defined Mn(II)-based products, most probably due to a thermal/acidic-promoted side reaction. So, once complex **2** was obtained and fully characterized, the next step was the reaction of complex **2** with radical **4**. However, prior to the reaction and to fully assess the stability of radical **4** in front complex **2**, a methylene chloride solution of radical **4** and complex **2** (1:1) was prepared and its evolution with time was followed by cyclic voltammetry. After 1 min, the cyclic voltammogram displays three electrochemical processes: two quasi-reversible processes at 350 mV and 860 mV and one strongly irreversible process at 1140 mV. As previously described [5], the first two electrochemical processes are attributed to the redox couples $[\text{Mn}_{12}\text{O}_{12}]/[\text{Mn}_{12}\text{O}_{12}]^-$ and $[\text{Mn}_{12}\text{O}_{12}]^+ / [\text{Mn}_{12}\text{O}_{12}]$, respectively. The last electrochemical process has been assigned to the irreversible oxidation of the nitroxide radical to an unstable oxoammonium ion [22] appearing at similar potential to that found for a free solution of radical **4**. After 9 min there is a displacement of ca. 30 mV of the anodic peaks corresponding to the oxidation process of **4**. No further evolution or changes on the voltammograms were observed. Therefore, this result shows the chemical stability of the $\text{Mn}_{12}\text{O}_{12}$ core under the reaction conditions.

To give more insight into the origin of the anodic peak displacement, a methylene chloride solution of radical **4** and complex **2** (1:1) was prepared and its evolution with time was followed by X-band EPR spectroscopy. Initially, the EPR spectrum shows the same pattern and hyperfine coupling constants than those observed for free radical **4**. After four days, the EPR spectrum of the mixture remains very similar with the only variation of a decrease of the hyperfine coupling constants associated to the nitrogen nuclei (Table 1). This fact indicates that there is a delocalization effect of the spin density onto the aromatic ring [23, 24] probably due to the enhancement of the electron-withdrawing capacity of the carboxylic group when passing from the protonated form of the free acid to the anionic carboxylate once linked to the Mn_{12} complex. The same arguments can

Table 1. EPR hyperfine coupling constants

Compd.	a_N	a_{Hortho}	a_{Hmeta}
4	11.57	2.13	0.92
3	11.70	2.09	0.84

be used to explain the displacement towards higher potentials of the redox process associated to the oxidation process of **4**.

From these results, it can be inferred that radical **4** quickly exchanges the pivalate ligand for the radical carboxylate and, secondly, its stability towards any side redox reaction. Therefore, Mn_{12} complex **3** was prepared by layering a dichloromethane solution of an excess (200%) of the acidic radical **4** and complex **2** with hexane. Complex **3** was collected as a microcrystalline brown-orange powder and fully characterized by elemental analysis, LDI/MALDI-TOF mass spectroscopy, FT-IR and UV-Vis spectroscopy, and SQUID measurements. It has to be emphasized that despite the use of recurrent crystallization experiments the obtaining of single crystals suitable for X-ray studies remained elusive. Elemental analysis, IR spectroscopy and the total absence of any signal in the 1H NMR spectrum, which is due to the fully paramagnetic nature of the complex, are consistent with a total replacement of the pivalate ligands by the carboxylate radicals.

Magnetochemical characterization

$[Mn_{12}O_{12}(O_2C^tBu)_{16}(H_2O)_4]$ (**2**). Complex **2** exhibits the characteristic single-molecule magnetism behavior of Mn_{12} complexes. Ac magnetic susceptibility data were obtained for a polycrystalline sample of complex **2** in the 1.8–10 K range with a 1 Oe ac field oscillating in the frequency range of 1–1000 Hz (see Fig. 2) and with an external magnetic field held at zero. Frequency-dependent signals in

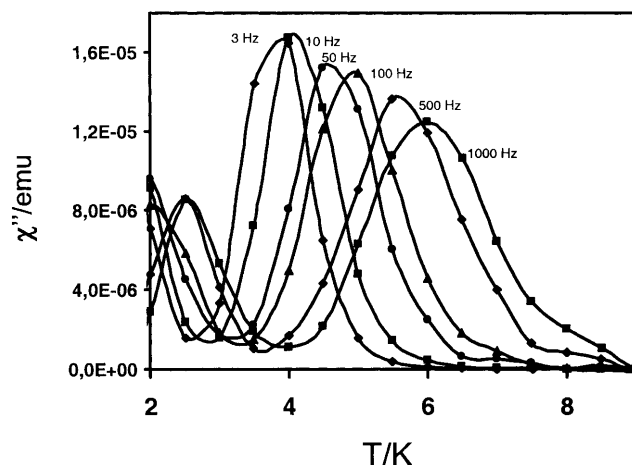


Fig. 2. Ac out-of-phase signals (χ'') of complex $[Mn_{12}O_{12}(O_2C^tBu)_{16}(H_2O)_4]$ **2**. The lines are visual guides

the out-of-phase ac magnetic susceptibility are seen, which indicates that complex **2** retains the single-molecule magnetic behavior. Remarkable is the observation of two frequency dependent peaks in the temperature range of 2–4 K and 4–6 K, as previously observed for other Mn_{12} complexes, which may be attributed to the presence of at least two different magnetization relaxation processes.

Magnetization relaxation times (τ) are obtained from the relationship $\omega\tau = 1$ at the maxima of the χ_M'' vs. temperature curves [25], which can be determined by fitting the χ_M'' vs. temperature data to a *Lorentzian* function. Indeed, the ac susceptibility data for complex **2** were least-squares fit to the *Arrhenius* law (Eq. 3):

$$\frac{1}{\tau} = \frac{1}{\tau_0} \exp(-U_{\text{eff}}/kT) \quad (3)$$

where U_{eff} is the effective anisotropy energy barrier, k is the *Boltzmann* constant and T is the temperature at which the maximum occurs. The least-squares fit of the ac susceptibility data for the low-temperature and high-temperature out-of-phase signals gave an energy barrier of 23.8 K and 58.1 K, with an attempt frequency of $1.0 \cdot 10^{-7}$ s and $8 \cdot 10^{-8}$ s, respectively.

Magnetization hysteresis data were obtained for a polycrystalline sample of complex **2** at three different temperatures between 1.8 and 2.5 K employing a SQUID magnetometer (see Fig. 3).

The sample is first magnetically saturated in a +2.0 T field, and then the field is swept down to −2.0 T, and cycled back to +2.0 T. As the field is decreased from +2.0 T, the first pronounced step appears at zero field consistently with the observation of two out-of-phase frequency dependent peaks in the ac magnetic susceptibility data. The lower effective barrier, corresponding to the low temperature peak, is still not active at the temperature of measure, and contributes with a superparamagnetic behavior at this temperature, that dominates the magnetic

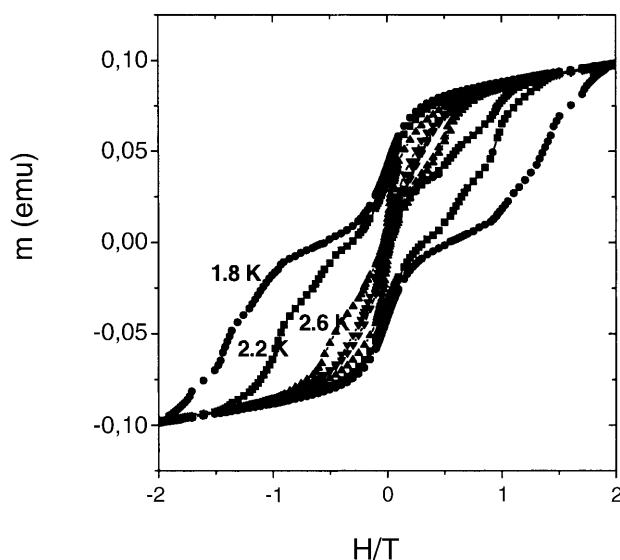


Fig. 3. Magnetization hysteresis loops measured at 1.8 K (●), 2.2 K (■), 2.6 K (▲) and 3.0 K (▼). The sample was aligned by external magnetic field and fixed with eicosane

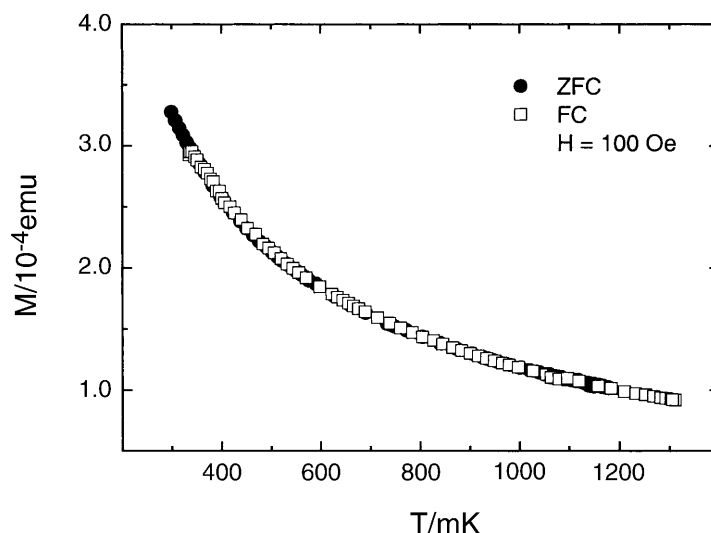


Fig. 4. ZFC-field cooled FC magnetization experiments at 100 Oe down to 300 mK for $[\text{Mn}_{12}\text{O}_{12}(\text{O}_2\text{CC}_6\text{H}_4\text{N}(\text{O}^\bullet)\text{tBu})_{16}(\text{H}_2\text{O})_4]$ complex **1c**

relaxation at zero field. In addition, there are successive steps observed at a field interval of approximately 4.5 kOe, which can be explained in terms of resonant spin tunneling relaxation.

$[\text{Mn}_{12}\text{O}_{12}(\text{O}_2\text{CC}_6\text{H}_4\text{N}(\text{O}^\bullet)\text{tBu})_{16}(\text{H}_2\text{O})_4]$ (**3**). Magnetic measurements were performed in the temperature range of 0.3 K to 20 K. The zero field cooled (ZFC)-field cooled (FC) magnetization experiments at 100 Oe down to 300 mK are shown in Fig. 4. As it can be observed, there is good matching between the experimental data of both, ZFC and FC magnetization, indicating that complex **3** exhibits a superparamagnetic behavior in all the temperature range studied.

Figure 5 shows the field dependence of the magnetization at five different temperatures ranging from 1.8 to 20 K where no hysteresis loop is observed even at the lowest temperature of 1.8 K. Fitting of the experimental data to the *Brillouin* function indicates that the ground state of the complex is $S = 2$.

To explain the resulting low effective magnetic moment, first it is convenient to revise the magnetic core of Mn_{12} clusters. Mn_{12} complex possesses a $[\text{Mn}_{12}(\mu_3\text{-O})_{12}]$ core comprising a central $[\text{Mn}^{\text{IV}}_4\text{O}_4]^{8+}$ cubane held within a non-planar ring of eight Mn^{III} ions. Assuming the presence of diamagnetic carboxylate ligands, Mn_{12} complexes must have a $S = 10$ state, which can be loosely described setting all the Mn^{III} spins up ($S = 8 \cdot 2 = 16$) and all the Mn^{IV} spins down ($S = 4 \cdot -3/2 = -6$). If we now include additional 16 free radicals ($S = 1/2$) from the peripheral ligation interacting antiferromagnetically with the Mn_{12} core ($S = 10$), a $S = 2$ magnetic ground state should result, as in fact it was experimentally observed. Assuming that complex **3** maintains constant the magnetic anisotropy arising from the single-ion zero-field splitting of Mn^{III} , the low $S = 2$ value may explain why no blocking temperature is observed. However, we cannot preclude that an hypothetical SMM behavior may remain hidden by the enhancement of the magnetic relaxation afforded by the paramagnetic ligands, as previously

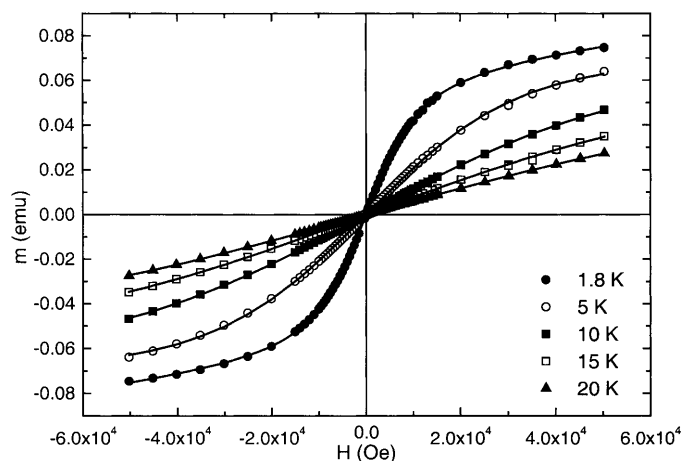


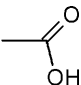
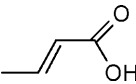
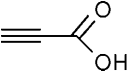
Fig. 5. Field strength dependence of the magnetization in the temperature range of 1.8–20 K showing the superparamagnetic behavior of a microcrystalline sample of complex **1c**. Solid lines represent the fit of experimental data to a *Brillouin* function assuming an $S = 2$ magnetic ground state

observed with the organic radical cation of a Mn_{12}^- complex [11]. Indeed, the presence of additional paramagnetic species may promote a fast magnetic relaxation process in spite the presence of an energy barrier for the interconversion from the *spin up* to the *spin down* state, which is expected to promote slow magnetization relaxation processes. Further high-field ESR experiments are currently underway to fully discard such possibility.

Conclusion

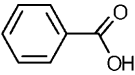
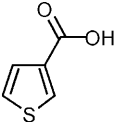
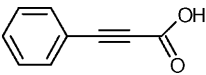
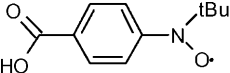
We have presented a new modified synthetic approach, based on the use of complex $[\text{Mn}_{12}\text{O}_{12}(\text{O}_2\text{C}^t\text{Bu})_{16}(\text{H}_2\text{O})_4]$ (**2**) as starting material, for the convenient synthesis of the new manganese complex $[\text{Mn}_{12}\text{O}_{12}(\text{O}_2\text{CC}_6\text{H}_4\text{N}(\text{O}^\bullet)\text{Bu})_{16}(\text{H}_2\text{O})_4]$ (**3**).

Table 2. Series of Mn_{12} complexes prepared following the modified synthetic approach based on the use of complex **2** as starting material

Ligand formula	Yield (%)	Complex formula
	96	$[\text{Mn}_{12}\text{O}_{12}(\text{O}_2\text{CH}_3)_{16}(\text{H}_2\text{O})_4] \cdot 4\text{H}_2\text{O} \cdot 2\text{CH}_3\text{CO}_2\text{H}$
	90	$[\text{Mn}_{12}\text{O}_{12}(\text{O}_2\text{CCH}=\text{CHCH}_3)_{16}(\text{H}_2\text{O})_4] \cdot \text{H}_2\text{O}$
	86	$[\text{Mn}_{12}\text{O}_{12}(\text{O}_2\text{CC}\equiv\text{CH})_{16}(\text{H}_2\text{O})_4] \cdot 4\text{H}_2\text{O}$

(continued)

Table 2 (continued)

Ligand formula	Yield (%)	Complex formula
	97	$[\text{Mn}_{12}\text{O}_{12}(\text{O}_2\text{CC}_6\text{H}_5)_{16}(\text{H}_2\text{O})_4]$
	91	$[\text{Mn}_{12}\text{O}_{12}(\text{O}_2\text{CC}_4\text{H}_3\text{S})_{16}(\text{H}_2\text{O})_4]$
	98	$[\text{Mn}_{12}\text{O}_{12}(\text{O}_2\text{CC}\equiv\text{CC}_6\text{H}_5)_{16}(\text{H}_2\text{O})_4] \cdot 4\text{H}_2\text{O}$
	78	$[\text{Mn}_{12}\text{O}_{12}(\text{O}_2\text{CC}_6\text{H}_4\text{N}(\text{O}^\bullet)\text{tBu})_{16}(\text{H}_2\text{O})_4]$

The preparation of complex **3** remained elusive with the conventional synthetic procedure shown in Eq. 2. Complex **3** bearing open-shell radical units was prepared to increase the total spin number of its ground state, and consequently to increase T_B , with the expectation that radical ligands may be coupled ferromagnetically with the Mn_{12} core. Unfortunately, magnetic measurements of complex **3** revealed that the sixteen radical carboxylate ligands interact antiferromagnetically with the Mn_{12} core to yield a $S=2$ magnetic ground state, which proved to be negative to achieve a SMM behavior. Finally, it is important to emphasize that this new synthetic approach not only allowed the preparation of complex **3** but other Mn_{12} complexes (shown in Table 2), otherwise unrealizable by direct replacement of the acetate groups of Mn_{12}Ac (**1**). Further work to fully characterize all the Mn_{12} complexes shown in Table 2 is currently in progress.

Experimental

Solvents were distilled prior to use. THF was distilled over sodium/benzophenone under Argon atmosphere whereas CH_2Cl_2 was distilled over P_2O_5 under nitrogen atmosphere. All the reagents were used as received. Microanalyses were performed by the Servei d'Anàlisi of the Universitat de Barcelona. Manipulations involving organometallic reagents were done using the standard *Schlenck* techniques. $[\text{Mn}_{12}\text{O}_{12}(\text{O}_2\text{CCH}_3)_{16}(\text{H}_2\text{O})_4] \cdot 4\text{H}_2\text{O} \cdot 2\text{CH}_3\text{CO}_2\text{H}$ (**1**) was prepared using the method originally described by *Lis* [20]. Radical 1-[*N*-*tert*-butyl-*N*-(oxy)amino]-4-benzoic radical (**4**) was prepared as previously described [26].

Physical measurements

DC magnetic measurements were collected on oriented powder samples restrained in eicosane to prevent torquing on a Quantum Design MPMS2 SQUID (rf) magnetometer equipped with a 5 T (50 kOe) magnet and capable of achieving temperatures from 1.8 to 350 K. Sample alignment in eicosane was performed while keeping the samples in a 5 T field at a temperature above the melting

point (312 K) of eicosane for 15 min, and then decreasing the temperature gradually to constrain the sample. Measurements below 1.8 K were performed in a SQUID (dc) magnetometer placed in a $^3\text{He} + ^4\text{He}$ dilution cryostat, which can achieve temperatures from 100 to 1500 mK. Cyclic voltammetry was carried out on a EG&G Instrument potentiostat/galvanostat, model 263A. Commercial tetrabutylammonium hexafluorophosphate was used as supporting electrolyte (0.1 M). A platinum spiral was used as the working electrode a platinum thread as the counter electrode and Ag/AgCl electrode as the reference electrode. EPR spectra were recorded on degassed solutions using a Bruker ESP-300E spectrometer operating in the X-band (9.3 GHz). Liquid state ^1H NMR spectra were recorded at room temperature on a Bruker Advance DPX 200 spectrometer operating at 200.13 MHz. IR spectra were taken on a Perkin Elmer 1600 FT by using the standard KBr dispersion method. Matrix Assisted LASER Desorption Ionization-Time of Flight (MALDI-TOF) mass spectra were recorded using a KRATOS ANALYTICAL KOMPACT MALDI-2 K-PROBE instrument, equipped with a nitrogen laser ($\lambda = 337$ nm) for the characterization of Mn_{12} complexes [27].

[Mn₁₂O₁₂(O₂C^tBu)₁₆(H₂O)₄] (2; C₈₀H₁₅₂O₄₈Mn₁₂)

To a slurry of complex **1** (1.0 g, 0.49 mmol) in 50 ml of toluene was added HO₂C^tBu (2.0 g, 19.6 mmol). The solution was allowed to stir overnight. Then, the mixture was concentrated under vacuum to remove the acetic acid. The resulting mixture were dissolved in toluene (50 ml), and then concentrated under vacuum. To fully substitute the acetate ligands, this procedure was repeated once more. The resulting brown semi-solid was recrystallized in acetonitrile. The resulting black crystals of **2** (1.0 g, 80%) were collected on a frit and washed with cold acetonitrile. ^1H NMR δ (CD₃CN, ppm): 15.3 (8H, H₂O), 11.6 (36H, axial ^tBu), 5.0 (36H, axial ^tBu), -2.0 (72H, equatorial ^tBu). FTIR (KBr, cm⁻¹): 3436 (broad, OH str); 2963 (medium, C-H str); 1587, 1558, 1529, 1426 (strong, CO₂⁻ str); 1484 (strong, ^tBu bend); 720 (medium, Mn₁₂O₁₂ str). LDI-TOF MS (negative-ion mode): $m/z = 2266$ [Mn₁₂O₁₂(O₂C^tBu)₁₄]⁻ (20%). Elemental analysis calcd for C₈₀H₁₅₂O₄₈Mn₁₂: C 37.80, H 5.98. Found: C 37.87, H 5.79.

[Mn₁₂O₁₂(O₂CC₆H₄N(O[•])^tBu)₁₆(H₂O)₄] (3; C₁₇₆H₂₁₆N₁₆O₆₄Mn₁₂)

To a solution of **2** (0.100 g, 0.04 mmol) in dichloromethane (5 ml) was added the desired carboxylic acid (1.6 mmol, 40 eq) and the resulting solution was stirred for few minutes. Recrystallization was achieved by slow diffusion of hexane (5 ml) into this solution. The resulting crystals or solids were collected, washed with hexane and dried on the frit orange-brown microcrystals (78%). FTIR (KBr, cm⁻¹): 3422 (broad, OH str); 2976 (medium, C-H str); 1594, 1545, 1404 (strong, CO₂⁻ str); 1430 (weak, ^tBu bend); 603 (medium, Mn₁₂O₁₂ bend). LDI-TOF MS (negative-ion mode): $m/z = 3558$ [Mn₁₂O₁₂(O₂CC₆H₄N(O[•])^tBu)₁₃]⁻ (20%). Elemental analysis calcd for C₁₇₆H₂₁₆N₁₆O₆₄Mn₁₂: C 49.86, H 5.10, N 5.29. Found: C 49.91, H 5.22, N 4.74.

Acknowledgments

This work was supported by the *Information Society Technologies* Programme of the European Commission, under project NANOMAGIQC, from DGI (MAT 2000-1388-C03-01), CIRIT (2001SGR 00362) and the 3MD Network of the TMR program of the E.U. (contract ERBFMRXCT 980181). Ph. G. is grateful to the CSIC and to the Région Languedoc-Roussillon for their financial support.

References

- [1] Leuenberger MN, Loss D (2001) *Nature* **40**: 789
- [2] Tejada J, Chudnovsky EM, Del Barco E, Hernández JM, Spiller TP (2000) *Nanotechnology* **12**: 181

- [3] Richter HJ (1999) *J Phys D: Appl Phys* **32**: R147
- [4] Sessoli R, Gatteschi D, Caneschi A, Novak M (1993) *Nature* **365**: 149
- [5] Sessoli R, Tsai H-K, Schake AR, Wang S, Vincent JB, Folting K, Gatteschi D, Christou G, Hendrickson DN (1993) *J Am Chem Soc* **115**: 1804
- [6] Aubin SMJ, Sun Z, Eppley HJ, Rumberger EM, Guzei IA, Folting K, Gantzel PK, Rheingold AL, Christou G, Hendrickson DN (2001) *Inorg Chem* **40**: 2127
- [7] Soler M, Artus P, Folting K, Huffman JC, Hendrickson DN, Christou G (2001) *Inorg Chem* **40**: 4902
- [8] Boskovic C, Pink M, Huffman JC, Hendrickson DN, Christou G (2001) *J Am Chem Soc* **123**: 9914
- [9] Artus P, Boskovic C, Yoo J, Streib WE, Brunel L-C, Hendrickson DN, Christou G (2001) *Inorg Chem* **40**: 4199
- [10] Eppley HJ, Tsai H-L, De Vries N, Folting K, Christou G, Hendrickson DN (1995) *J Am Chem Soc* **117**: 301
- [11] Takeda K, Awaga K (1997) *Phys Rev B* **56**: 14560
- [12] Aubin SMJ, Dilley NR, Wemple MW, Maple MB, Christou G, Hendrickson DN (1998) *J Am Chem Soc* **120**: 839
- [13] Aubin SMJ, Dilley NR, Pardi L, Kryzstek J, Wemple MW, Brunel L-C, Maple MB, Christou G, Hendrickson DN (1998) *J Am Chem Soc* **120**: 4991
- [14] Sun Z, Grant CM, Castro SL, Hendrickson DN, Christou G (1998) *Chem Commun* 721
- [15] Castro SL, Sun Z, Grant CM, Bollinger JC, Hendrickson DN, Christou G (1998) *J Am Chem Soc* **120**: 2365
- [16] Barra A-L, Debrunner P, Gatteschi D, Schulz CE, Sessoli R (1996) *Europhys Lett* **35**: 133
- [17] Sangregorio C, Ohm T, Paulsen C, Sessoli R, Gatteschi D (1997) *Phys Rev Lett* **78**: 4645
- [18] Barra A-L, Caneschi A, Cornia A, Fabrizi de Biani F, Gatteschi D, Sangregorio C, Sessoli R, Sorace L (1999) *J Am Chem Soc* **121**: 5302
- [19] Ruiz-Molina D, Christou G, Hendrickson DN (2002) *Single-Molecule Magnets*. In: Sasabe H (ed) *Hyperstructured Materials*, Gordon-Breach, in press
- [20] Lis T (1980) *Acta Cryst* **B36**: 2042
- [21] Chrysiuk E, Jusoh A, Santafianos D, Williams A (1986) *J Chem Soc, Perkin Trans 2*, 163
- [22] Baur JE, Wang S, Brandt MC (1996) *Anal Chem* **68**: 3815
- [23] Shultz DA, Gwaltney KP, Lee H (1998) *J Org Chem* **63**: 769
- [24] Barbarella G, Rassat A (1969) *Bull Soc Chim Fr* 2378
- [25] Paulsen C, Park J-G. In: *Quantum Tunneling of Magnetization-QTM'94*; Gunther L, Barbara B, Kluwer Academic Publishers, Dordrecht, 1995; pp 171–188
- [26] MasPOCH D, Catala L, Gerbier Ph, Ruiz-Molina D, Vidal-Gancedo J, Wurst K, Rovira C, Veciana J (2002) *Chem Eur J*, in press
- [27] Ruiz-Molina D, Gerbier Ph, Rumberger E, Amabilino DB, Guzei IA, Folting K, Huffman JC, Rheingold A, Christou G, Veciana J, Hendrickson DN (2002) *J Mater Chem* **12**: 1152